The complement inhibitory protein DAF (CD55) suppresses T cell immunity in vivo

Jianuo Liu,[1] Takashi Miwa,[1] Brendan Hilliard,[2] Youhai Chen,[2] John D. Lambris,[2] Andrew D. Wells,[2,3] and Wen-Chao Song[1]

[1]Institute for Translational Medicine and Therapeutics and Department of Pharmacology, [2]Department of Pathology and Laboratory Medicine, and [3]Children's Hospital of Philadelphia, University of Pennsylvania School of Medicine, Philadelphia, PA 19104

Decay-accelerating factor ([DAF] CD55) is a glycosylphosphatidylinositol-anchored membrane inhibitor of complement with broad clinical relevance. Here, we establish an additional and unexpected role for DAF in the suppression of adaptive immune responses in vivo. In both C57BL/6 and BALB/c mice, deficiency of the Daf1 gene, which encodes the murine homologue of human DAF, significantly enhanced T cell responses to active immunization. This phenotype was characterized by hypersecretion of interferon (IFN)-γ and interleukin (IL)-2, as well as down-regulation of the inhibitory cytokine IL-10 during antigen restimulation of lymphocytes in vitro. Compared with wild-type mice, Daf1$^{-/-}$ mice also displayed markedly exacerbated disease progression and pathology in a T cell–dependent experimental autoimmune encephalomyelitis (EAE) model. However, disabling the complement system in Daf1$^{-/-}$ mice normalized T cell secretion of IFN-γ and IL-2 and attenuated disease severity in the EAE model. These findings establish a critical link between complement and T cell immunity and have implications for the role of DAF and complement in organ transplantation, tumor evasion, and vaccine development.

CORRESPONDENCE
Wen-Chao Song:
Song@spirit.gcrc.upenn.edu

Abbreviations used: DAF, decay-accelerating factor; EAE, experimental autoimmune encephalomyelitis; GPI, glycosylphosphatidylinositol; GVBS, gelatin veronal-buffered saline; MOG, myelin oligodendrocyte glycoprotein; SEB, Staphylococcus enterotoxin B; T reg cell, T regulatory cell.

Decay-accelerating factor ([DAF] CD55) is a glycosylphosphatidylinositol (GPI)-anchored membrane inhibitor of complement (1, 2). It inhibits complement activation by interfering with the function of C3 and C5 convertases in both the classical and alternative pathways (1, 2). Clinically, DAF has been found to be deficient on affected blood cells and platelets of paroxysmal nocturnal hemoglobinuria patients, contributing to the heightened sensitivity of such cells to autologous complement attack (3–5). In many types of human carcinomas, on the other hand, up-regulation of DAF is observed, suggesting that circumvention of complement-mediated tumoricidal activity may constitute a tumor evasion mechanism (6–8). DAF is also a therapeutic target in the setting of xenotransplantation. Transgenic expression of human DAF on porcine endothelial cells is used as a strategy to thwart complement-mediated hyperacute rejection in pig to primate xenotransplantation (9–11).

A number of previous studies have suggested that DAF may participate in T cell function as a GPI molecule in lipid rafts (12–14). Additionally, DAF has been identified as a ligand for an activation-associated, seven-transmembrane lymphocyte receptor, CD97 (15–18); however, the significance of DAF–CD97 interaction remains unknown. We previously generated, by gene targeting, a mouse that is deficient in the Daf1 gene that encodes the murine homologue of human DAF (19). As expected, we found that Daf1$^{-/-}$ mice are more susceptible to complement-mediated inflammatory injury (19–21). Unexpectedly, when bred onto the autoimmune disease–prone MRL/lpr background, Daf1$^{-/-}$ mice developed exacerbated lymphadenopathy and splenomegaly (22), raising the possibility that DAF may also function as a negative regulator of adaptive immunity in vivo. In this study, we investigated this possibility by studying the T cell responses of WT and Daf1$^{-/-}$ mice to active immunization. We show that deficiency of Daf1 significantly enhanced T cell response to active immunization via a complement-dependent mechanism. Thus, our findings identify DAF as a key molecule that regulates the interplay between complement and T cell immunity in vivo. This conclusion has implications for the immunobiology and therapeutics of DAF in organ transplantation, tumor evasion, and vaccine development.

The Journal of Experimental Medicine

RESULTS

Daf1$^{-/-}$ mouse lymphocytes responded more vigorously to antigen restimulation

To evaluate T lymphocyte immunity in Daf1$^{-/-}$ mice, we immunized C57BL/6-Df1$^{-/-}$ and C57BL/6 WT mice with OVA in the presence of CFA. 12 d later, LNs were isolated and cells were prepared and restimulated with OVA in culture. Fig. 1, A and B, shows that compared with cells from WT mice, LN cells from Daf1$^{-/-}$ mice proliferated more vigorously and secreted more IFN-γ. Restimulation of LN cells from Daf1$^{-/-}$ mice immunized with a different antigen, myelin oligodendrocyte glycoprotein (MOG) peptide (MOG 38–50) bearing a T cell epitope (23), produced similar results, with Daf1$^{-/-}$ cells displaying increased proliferation and IFN-γ secretion compared with WT cells (Fig. 1, C and D). With both antigens, similar results were obtained when splenocytes alone were prepared from the immunized mice and restimulated (not depicted). Therefore, we combined LN cells and splenocytes in subsequent experiments unless specified otherwise.

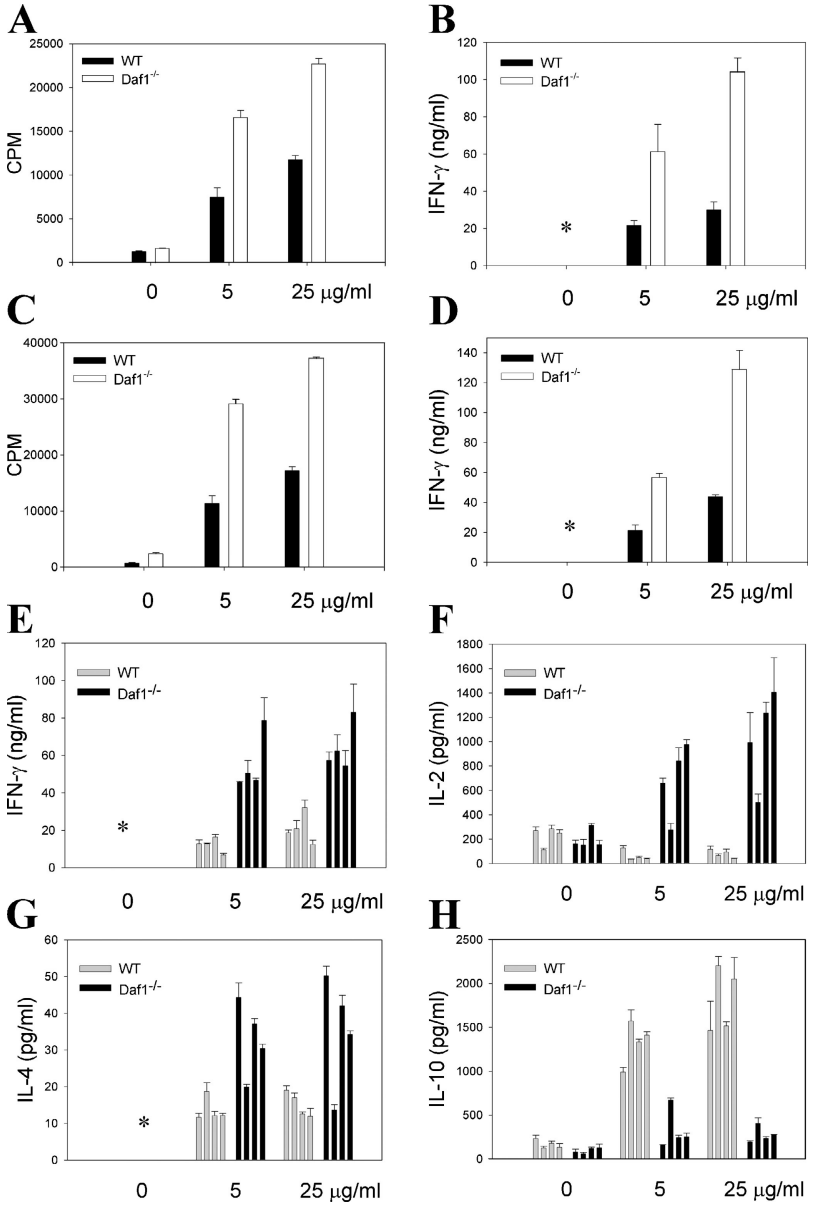

Figure 1. Responses of C57BL/6 WT and Daf1$^{-/-}$ mouse lymphocytes to antigen restimulation. (A–D) LN cells from four mice in each group were pooled and restimulated with antigen in vitro (in triplicate assays) 12 d after immunization with OVA (A and B) or MOG 38–50 (C and D). Cell proliferation (A and C) and IFN-γ production (B and D) were determined. Similar results were obtained with splenocytes (not depicted). Results are representative of three independent experiments. (E–H) Spleen and LN cells from each mouse were combined and restimulated with antigen in vitro (in triplicate assays) 60 d after immunization with OVA, and the production levels of four cytokines were determined (each bar represents a single mouse, and four mice were used in each group). The x axis represents antigen concentration during restimulation assays. Asterisks designate levels that were below the detection limits. Results are representative of three independent experiments.

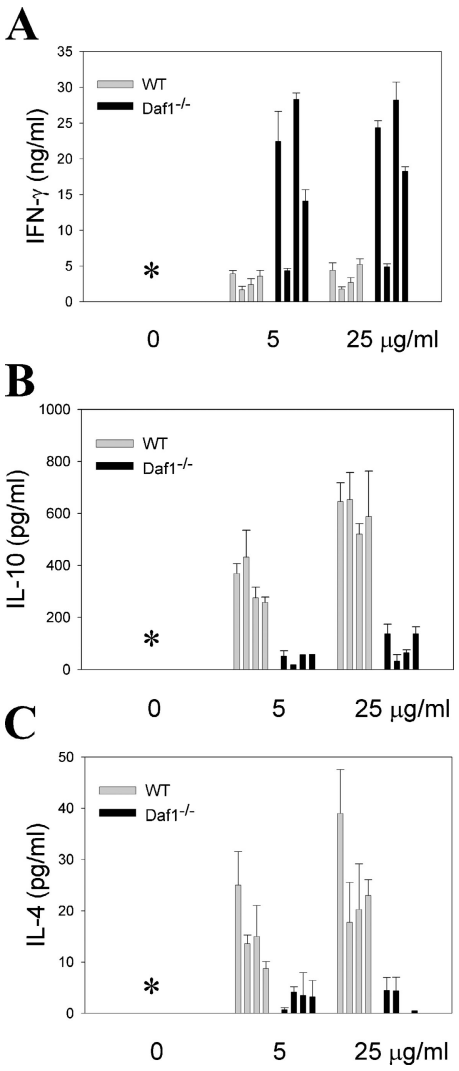

Figure 2. Responses of BALB/c WT and Daf1$^{-/-}$ mouse lymphocytes to antigen restimulation. Spleen and LN cells from each mouse were combined and restimulated with OVA in vitro (in triplicate assays) 12 d after immunization, and cytokine production was determined (each bar represents a single mouse, and four mice were used in each group). The x axis represents OVA concentration used for restimulation. Asterisks designate levels that were below the detection limits. Results are representative of two independent experiments.

To determine if the increased restimulation response persists in memory T cells of Daf1$^{-/-}$ mice, we immunized C57BL/6-Df1$^{-/-}$ and C57BL/6 WT mice with OVA and tested the recall responses of their lymphocytes 60 d later. Fig. 1 E shows that cultured lymphocytes from Daf1$^{-/-}$ mice again secreted significantly increased amounts of IFN-γ, as noted in the previous experiment, and they also produced higher levels of IL-2 and IL-4 (Fig. 1, F and G). On the other hand, we found that the production of the inhibitory cytokine IL-10 by the Daf1$^{-/-}$ cells was markedly reduced (Fig. 1 H).

Next, we investigated whether the effect of Daf1 deficiency on the restimulation response of mouse T cells is specific to C57BL/6 mice. Using a procedure similar to the one outlined above, we immunized BALB/c-Daf1$^{-/-}$ and BALB/c WT mice with OVA and determined the restimulation responses of their lymphocytes after 12 d. Fig. 2 shows that as was the case with the C57BL/6-Df1$^{-/-}$ mice, restimulated lymphocytes from BALB/c-Daf1$^{-/-}$ mice displayed increased IFN-γ and decreased IL-10 production as compared with those of WT control animals (Fig. 2, A and B). However, in contrast to C57BL/6-Df1$^{-/-}$ mice, the production of IL-4 by restimulated BALB/c-Daf1$^{-/-}$ mouse T cells was significantly reduced. Thus, there appears to be a strain difference between C57BL/6 and BALB/c mice in that Daf1 deficiency in BALB/c mice caused a more polarized Th1 cell response to immunization.

Enhanced restimulation response by Daf1$^{-/-}$ lymphocytes tracks with T cells

To determine if the hyperresponse phenotype of Daf1$^{-/-}$ mouse lymphocytes was caused by altered APC function or was associated with T cells, we purified CD4$^+$ T cells and APCs from OVA-immunized C57BL/6-Df1$^{-/-}$ and

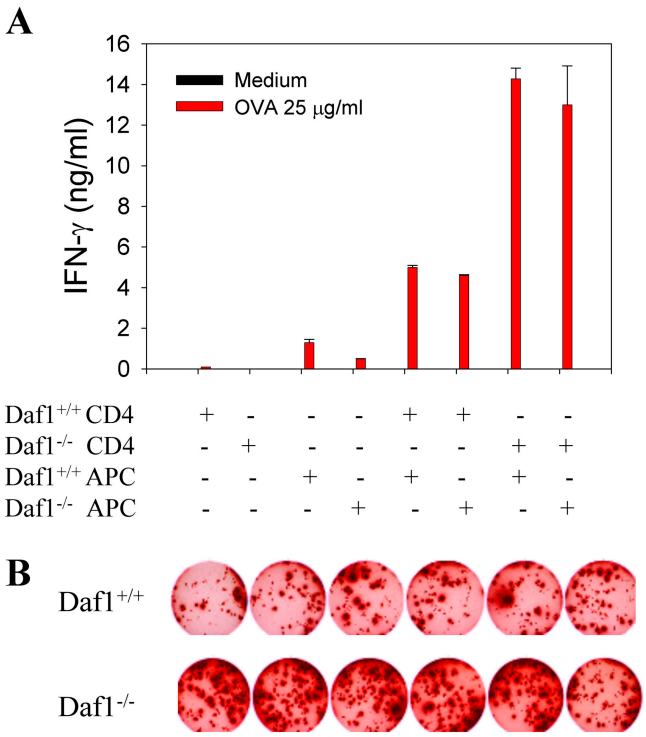

Figure 3. Enhanced restimulation response of Daf1$^{-/-}$ spleen and LN cell tracks with T cells. (A) CD4$^+$ T cells and APCs were purified from spleen and LN cells of immunized C57BL/6 WT and Daf1$^{-/-}$ mice (pooled from four animals in each group and immunized with OVA for 12 d) and cross-matched in antigen-restimulation assays in vitro (2×10^5 CD4$^+$ cells/well or 10^6 APCs/well alone or in combination with or without 25 μg/ml OVA, triplicate assays for each treatment). IFN-γ levels in the cell culture medium were assayed after 48 h of culture. B shows ELISPOT assays of IFN-γ–secreting T cells in lymphocyte cultures of C57BL/6 WT and Daf1$^{-/-}$ mice. Spleen and LN cells from immunized C57BL/6 WT and Daf1$^{-/-}$ mice (pooled from four animals in each group and immunized with OVA for 12 d) were restimulated with 25 μg/ml OVA for 40 h (six replicate assays, 10^5cells/well). Results are representative of two independent experiments.

C57BL/6 WT mice and cross-matched them in the restimulation assay. Fig. 3 A shows that the genotype of APCs had no impact on IFN-γ production by either WT or Daf1$^{-/-}$ CD4$^+$ T cells, whereas Daf1$^{-/-}$ CD4$^+$ T cells secreted more IFN-γ than WT CD4$^+$ T cells regardless of whether they were mixed with WT or Daf1$^{-/-}$ APCs. Using ELISPOT, we also found that there were significantly more IFN-γ–secreting T cells in the lymphocyte cultures of Daf1$^{-/-}$ mice than in those of WT mice (Fig. 3 B). These results suggested that clonal expansion and/or survival of antigen-primed CD4$^+$ cells was enhanced in Daf1$^{-/-}$ mice in vivo.

Hyper T cell response in Daf1$^{-/-}$ mice was largely dependent on complement

Next, we investigated if the hyper response of Daf1$^{-/-}$ mouse T cells to immunization was caused by the lack of DAF available to function as a complement inhibitor. If this were the case, removal of the complement system from Daf1$^{-/-}$ mice should attenuate or reverse the phenotype. To test this hypothesis, we produced C57BL/6-Df1$^{-/-}$-C3$^{-/-}$ mice by crossing Daf1$^{-/-}$ mice with C3$^{-/-}$ mice. We then compared the memory T cell response to antigen restimulation in WT, C3$^{-/-}$, Daf1$^{-/-}$, and Daf1$^{-/-}$-C3$^{-/-}$ mice using IFN-γ and IL-2 secretion as readouts. As expected, lymphocytes from Daf1$^{-/-}$ mice secreted much higher levels of IFN-γ and IL-2 than those of WT mice (Fig. 4, A and B). Significantly, we found that deletion of the C3 gene from Daf1$^{-/-}$ mice normalized IFN-γ and IL-2 secretion such that the levels of these cytokines produced by Daf1$^{-/-}$-C3$^{-/-}$ lymphocytes were similar to those of WT cells (Fig. 4, A and B). The same result was noted in ELISPOT assays of IFN-γ–secreting T cells in lymphocyte cultures of these mice (Fig. 4, C and D). In contrast to the clear reversing effect on IFN-γ and IL-2 production, however, C3 deficiency did not consistently correct the IL-10 defect of Daf1$^{-/-}$ mice (not depicted). These results suggested that hypersecretion of

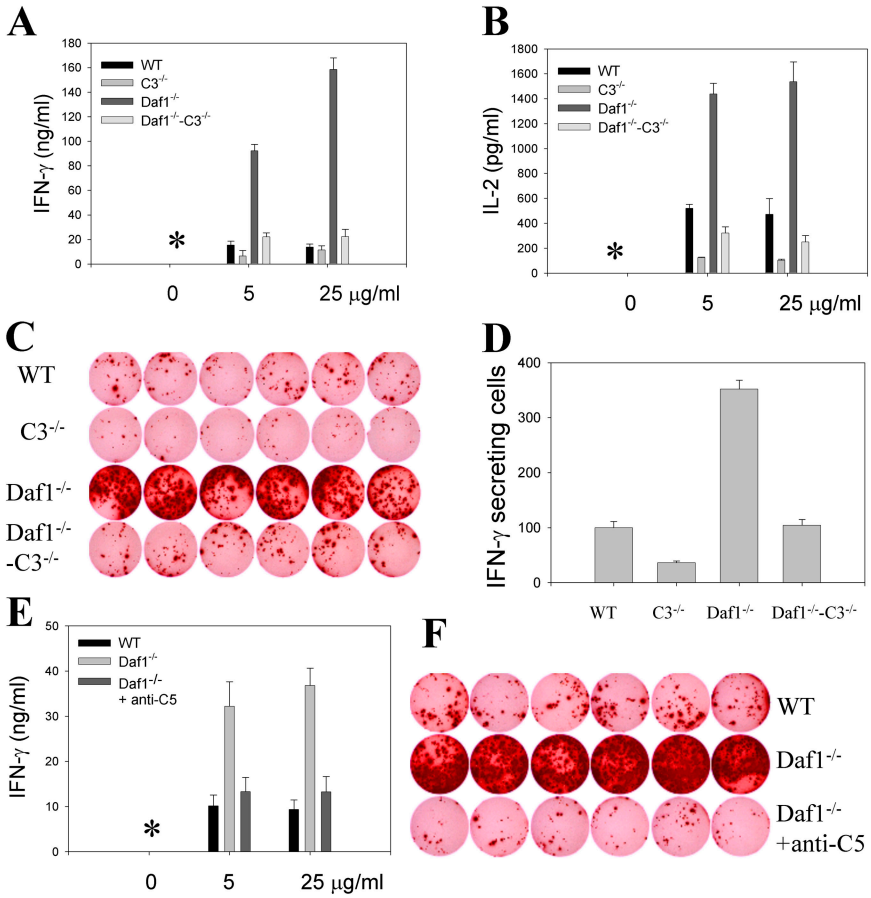

Figure 4. Hyper T cell response in Daf1$^{-/-}$ mice is largely dependent on complement. In the experiment shown in A–D, C57BL/6 WT, C3$^{-/-}$, Daf1$^{-/-}$, and Daf1$^{-/-}$-C3$^{-/-}$ mice were immunized with OVA. After 105 d, spleen and LN cells (pooled from four animals in each group) were restimulated in vitro (triplicate wells) and assayed for IFN-γ (A) and IL-2 (B) production. The frequency of IFN-γ–secreting T cells in the lymphocyte cultures was also determined by ELISPOT (C; six replicate assays, 10^5 cells/well, stimulated with 25 μg/ml OVA for 40 h). The average number of IFN-γ–secreting T cells per well is shown in D. Results are representative of two independent experiments. Experiments using splenocytes or LN cells alone gave similar results to those shown in A and B (not depicted). In the experiments shown in E and F, C57BL/6-Df1$^{-/-}$ mice were treated with an anti-C5 mAb or an isotype-matched IgG control antibody. As another control, C57BL/6 WT mice were also treated with the isotype-matched IgG. 12 d after immunization, spleen and LN cells (pooled from four mice in each group) were restimulated with 25 μg/ml OVA in culture for 40 h. IFN-γ production was assessed by ELISA (E; triplicate wells) or ELISPOT (F; six replicate wells at 10^5 cells/well).

IFN-γ by Daf1$^{-/-}$ mouse T cells was largely dependent on a functional complement system but was probably not secondary to the defect in IL-10 production. Because DAF regulates C3 activation by inhibiting both the classical pathway C3 convertase C4b2a and the alternative pathway C3 convertase C3bBb, it remains to be determined by which pathway C3 was activated in the Daf1$^{-/-}$ mice and whether C4 also plays a critical role in producing the observed cellular immunity phenotype in Daf1$^{-/-}$ mice.

It is of interest that compared with WT cells, there was a reduction in IFN-γ and IL-2 production by C3$^{-/-}$ mouse T cells (Fig. 4, A–D). This suggested that complement may play an adjuvant role in WT mice as well in facilitating T cell responses to active immunization. It is also notable that Daf1$^{-/-}$-C3$^{-/-}$ mouse T cells produced more IFN-γ and IL-2 than C3$^{-/-}$ mouse T cells (Fig. 4, A–D). This implied that Daf1 deficiency rendered T cells more responsive even in the absence of C3, suggesting the existence of a separate, C3-independent mechanism of T cell regulation by DAF. It is clear, however, that the putative C3-independent mechanism only played a marginal role in the Daf1$^{-/-}$ mouse phenotype under study.

To better understand the complement-dependent mechanism of T cell regulation by Daf1, we depleted C5 in C57BL/6-Df1$^{-/-}$ mice by administering an anti-C5 mAb (24). We then investigated the effect of C5 depletion on IFN-γ production by Daf1$^{-/-}$ mouse T cells in response to antigen restimulation in the OVA immunization model. We found that as with C3 gene inactivation in Daf1$^{-/-}$-C3$^{-/-}$ mice, C5 depletion in Daf1$^{-/-}$ mice also rescued their hyper T cell response phenotype (Fig. 4, E and F). This result implicated the anaphylatoxin C5a and/or the lytic pathway effector C5b-9 as the principal mediator(s) responsible for the observed Daf1$^{-/-}$ mouse phenotype.

Daf1$^{-/-}$ but not Daf1$^{-/-}$-C3$^{-/-}$ mice developed exacerbated experimental autoimmune encephalomyelitis (EAE)

To further confirm the inhibitory effect of DAF on T cell immunity, we studied the sensitivity of Daf1$^{-/-}$ mice to EAE induced by a MOG peptide (MOG 38–50), which bears a T cell epitope. Although complement is involved in some experimental models of EAE, as recently demonstrated for EAE induction by recombinant MOG in CD59a knockout mice (25), a previous study showed that EAE disease in mice induced by a closely related MOG peptide, MOG 35–55, was mainly T cell driven and independent of complement (26). We found that Daf1$^{-/-}$ mice immunized with MOG 38–50 developed a markedly exacerbated disease phenotype compared with similarly treated WT mice (Fig. 5). This was indicated by an increased average daily clinical score after disease onset (Fig. 5 A) and a higher endpoint mortality rate (80 vs. 10%; Table I) in the Daf1$^{-/-}$ group. Histologically, Daf1$^{-/-}$ mouse spinal cord sections had more abundant inflammatory infiltrates (Fig. 5, B–E) and a higher

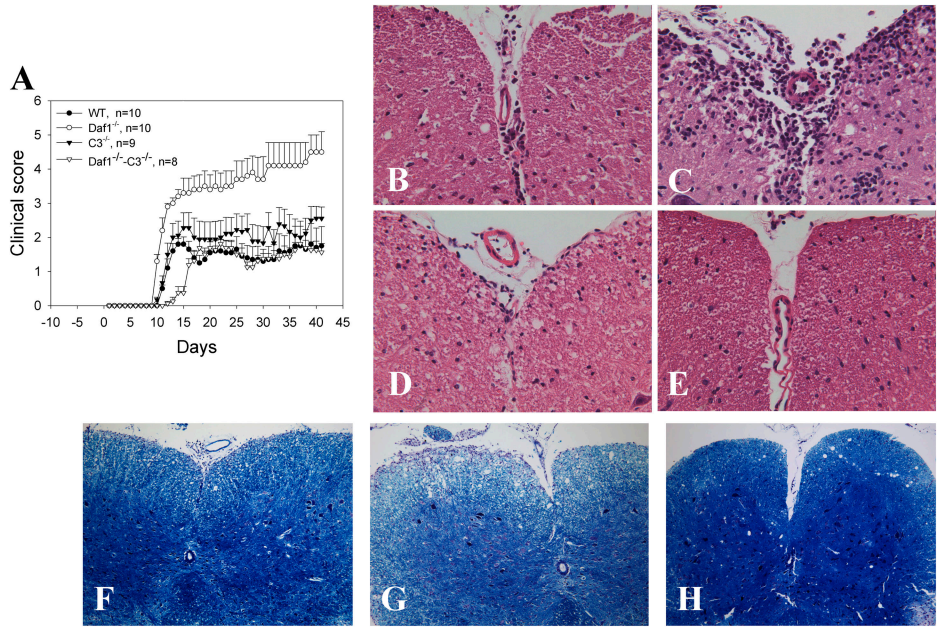

Figure 5. Daf1$^{-/-}$ but not Daf1$^{-/-}$-C3$^{-/-}$ mice developed exacerbated EAE. MOG 38–50 was used to induce EAE in groups of C57BL/6 WT, C3$^{-/-}$, Daf1$^{-/-}$, and Daf1$^{-/-}$-C3$^{-/-}$ mice. Compared with WT mice, Daf1$^{-/-}$ but not Daf1$^{-/-}$-C3$^{-/-}$ mice developed markedly exacerbated EAE disease (A). There was no significant difference between WT and C3$^{-/-}$ mice in daily clinical scores. One animal each in the WT and C3$^{-/-}$ group died, at days 36 and 14, respectively. 8 of the 10 animals in the Daf1$^{-/-}$ group died, 1 each at days 16, 25, 31, 36, 37, and 39, and 2 at day 35. B–E show representative histological pictures of spinal cords of WT (B), Daf1$^{-/-}$ (C), C3$^{-/-}$ (D), and Daf1$^{-/-}$-C3$^{-/-}$ (E) mice harvested from a separate experiment at 15 d after disease induction, demonstrating that there were significantly more inflammatory cell infiltrates in the Daf1$^{-/-}$ mouse spinal cords (a magnification of 400). F–H show that compared with that of WT (F) and Daf1$^{-/-}$-C3$^{-/-}$ (H) mice, the spinal cords of Daf1$^{-/-}$ (G) mice stained less intensely with luxol fast blue, suggesting increased demyelination (a magnification of 100).

Table I. Daf1$^{-/-}$ mice developed exacerbated EAE

Genotype	Incidence	Mortality	Days of onset[a]	Maximum disease score[a]
Daf1$^{+/+}$	10/10 (100%)	1/10 (10%)	11.3 ± 0.67	3.0 ± 1.1
Daf1$^{-/-}$	10/10 (100%)	8/10 (80%)	10.6 ± 0.70	4.6 ± 0.8
C3$^{-/-}$	9/9 (100%)	1/9 (11%)	10.9 ± 0.78	3.1 ± 0.9
Daf1$^{-/-}$-C3$^{-/-}$	8/8 (100%)	0/8 (0%)	15.0 ± 1.51	2.2 ± 0.59

[a]Mean ± SD.

degree of demyelination (Fig. 5, F–H). Deficiency of C3 from WT mice did not significantly attenuate EAE disease severity, whereas deficiency of C3 in Daf1$^{-/-}$ mice rescued the enhanced EAE disease phenotype (Fig. 5 and Table I). Thus, in this prototypical T cell–mediated autoimmune disease model, Daf1$^{-/-}$ but not Daf1$^{-/-}$-C3$^{-/-}$ mice had markedly exacerbated disease progression and pathology. These results are in agreement with in vitro assays of Daf1$^{-/-}$ mouse T cell function and highlight the relevance of our findings in a pathophysiological setting.

Daf1$^{-/-}$ mouse T cells responded similarly to superantigen stimulation and had no defect in T regulatory cells (T reg cells)

Several mechanisms, not mutually exclusive of one another, may underlie the observed hyper T cell response phenotype of Daf1$^{-/-}$ mice. These include enhanced sensitivity of T cells to activation stimuli, enhanced clonal expansion, and/or diminished contraction of the antigen-specific T cell pool and decreased T reg cell number and/or activity. To determine if Daf1$^{-/-}$ mouse T cells are intrinsically more responsive to activation stimuli, we stimulated splenocytes from C57BL/6 WT and Daf1$^{-/-}$ mice with the bacterial superantigen Staphylococcus enterotoxin B (SEB) and examined their proliferative responses, CD69 expression, and IFN-γ production. We detected no significant differences between the WT and Daf1$^{-/-}$ mice in these assays (Fig. 6, A–D). In separate experiments, we also observed no significant difference in either the number or function of the naturally occurring T reg cells in naive C57BL/6 and Daf1$^{-/-}$ mice (Fig. 6, E–G).

DISCUSSION

Here we demonstrated, both by in vitro assays and by a T cell–mediated autoimmune disease model, that deficiency of DAF in mice caused a hyper T cell response to active immunization. Daf1$^{-/-}$ T cells proliferated more vigorously and secreted more IFN-γ in response to antigen restimulation, and Daf1$^{-/-}$ mice developed markedly exacerbated EAE disease when immunized with a T cell epitope-bearing MOG peptide. Although our data revealed a potential C3-independent effect of Daf1 on T cell function that warrants further investigation, this C3-independent mechanism contributed marginally to the Daf1$^{-/-}$ mouse phenotype under study. Instead, the inhibitory effect of Daf1 on T cell immunity in this model appeared to be largely indirect and mediated by complement, as IFN-γ assays determined that inactivation of the C3 gene or depletion of C5 protein from Daf1$^{-/-}$ mice rescued the hyper T cell response phenotype. C3 deficiency also reversed EAE disease exacerbation in Daf1$^{-/-}$ mice. Although the role of complement as a natural adjuvant in B cell priming and memory maintenance is well recognized (27–29), recently, evidence has emerged that suggests that complement may also play an instrumental role in optimizing T cell response to viral or allogeneic antigens (30–33). Our finding that DAF, a GPI-anchored membrane protein known for its complement-inhibiting activity, negatively regulates T cell immunity is in accord with this emerging concept and suggests that complement regulatory proteins may significantly affect the interplay between complement and T cell immunity in vivo.

The fact that increased IFN-γ and decreased IL-10 production was observed in both C57BL/6-Daf1$^{-/-}$ and BALB/c-Daf1$^{-/-}$ mice strongly suggests that the observed abnormality in T cell immune response was caused by Daf1 deficiency and not by genetic background differences between WT and Daf1$^{-/-}$ mice. Notwithstanding this observation, we found that Daf1 deficiency had an opposing influence on IL-4 production by activated T cells in C57BL/6 and BALB/c mice. Consequently, Daf1 deficiency in BALB/c mice produced a hyper T cell response that was also markedly biased toward a Th1 cell phenotype. This divergent effect of Daf1 deficiency on IL-4 production likely reflected intrinsic differences in T cell immunity between the two mouse strains. The BALB/c strain of mice is well known for its tendency to mount a stronger Th2 cell immune response, and strain-dependent manifestations of phenotypes have been documented in other immune regulatory gene knockout studies (34, 35). For example, deletion of the programmed cell death-1 immunoinhibitory coreceptor gene caused autoimmune dilated cardiomyopathy in BALB/c but not C57BL/6 mice (35).

Our data indicate that augmented T cell response to antigen immunization in Daf1$^{-/-}$ mice is not caused by enhanced susceptibility of the T cells to activation stimuli, as WT and mutant mouse splenocytes responded similarly to activation by the bacterial superantigen SEB (Fig. 6, A–D). DAF is widely expressed on peripheral tissues as well as on T and B lymphocytes, macrophages, and dendritic cells (1, 2, 36, 37). It is therefore important to elucidate the mechanism(s) by which DAF suppresses T cell immunity in vivo. Although we found that Daf1$^{-/-}$ APCs functioned normally during antigen restimulation assays in vitro (Fig. 3 A), the responses of Daf1$^{-/-}$ T cells and APCs in vivo during the

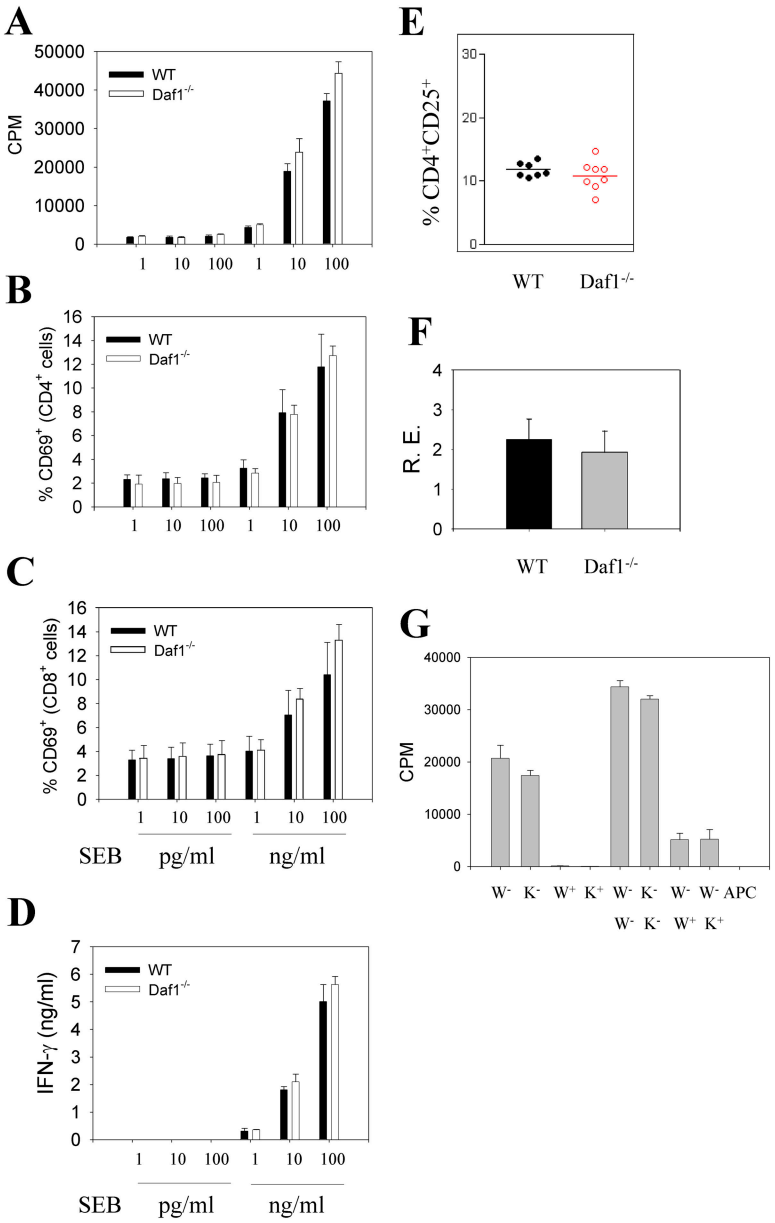

Figure 6. Daf1$^{-/-}$ mouse T cells responded similarly to SEB stimulation and had no defect in T reg cells. In the experiments shown in A–D, splenocytes from C57BL/6 WT and Daf1$^{-/-}$ mice ($n = 4$ mice in each group) were stimulated with SEB at the indicated concentrations and their proliferative response (A), CD69 expression on CD4$^+$ (B) and CD8$^+$ (C) T cells, and IFN-γ production (D) were compared. No significant difference was detected between the two groups in any of the measurements. Results are representative of two independent experiments. E and F show that there was no significant difference between WT and Daf1$^{-/-}$ mice in the number of naturally occurring T reg cells. Percentage of CD25$^+$ cells among spleen CD4$^+$ T cells was determined by FACS analysis in seven WT and eight Daf1$^{-/-}$ mice (E). Foxp3 expression in purified spleen CD4$^+$ T cells ($n = 3$ samples in each group, with each sample representing splenocytes pooled from two mice before CD4$^+$ cell selection) was determined by real-time RT-PCR (F). Foxp3 levels are shown as relative expression (R.E.) to the housekeeping gene L32. G shows that there was no difference between CD4$^+$ CD25$^+$ T cells from WT (W) or Daf1$^{-/-}$ (K) mice in their ability to inhibit anti-CD3–stimulated proliferation of CD4$^+$ CD25$^-$ T cells. W$^-$, CD4$^+$ CD25$^-$ T cells from WT; K$^-$, CD4$^+$ CD25$^-$ T cells from Daf1$^{-/-}$; W$^+$, CD4$^+$ CD25$^+$ T cells from WT; K$^+$, CD4$^+$ CD25$^+$ T cells from Daf1$^{-/-}$; APC, irradiated WT splenocytes.

priming phase of immunization are yet to be assessed. Such a question might be addressed by T cell adoptive transfer experiments using TCR transgenic mice carrying either a normal or mutated Daf1 gene. It is possible that DAF deficiency in peripheral tissues (e.g., skin) enhances complement activation and promotes local inflammation at the immunization sites, creating a more favorable environment for APC maturation and/or antigen capture and presentation. An alternative but not mutually exclusive hypothesis is that in the setting of active immunization, a lack of DAF leads to enhanced systemic inflammation and generation of a cytokine milieu that favors the survival of antigen-primed T cells. Both hy-

potheses are consistent with the demonstrated requirement of C5, a critical complement protein that when activated, gives rise to the anaphylatoxin C5a and the lytic pathway effector C5b-9 in the development of the hyper T cell response phenotype of the mutant mice (Fig. 4, E and F).

Another potential mechanism for increased T cell response to antigen immunization in Daf1$^{-/-}$ mice is decreased T reg cell number or function (38). T reg cells suppress immune responses to self- and nonself antigens (38). Two major T reg cell populations have been described so far: naturally occurring T reg cells and IL-10–secreting T reg cells (38). Both types of T reg cells express CD25 on their surface, but only the naturally occurring T reg cells express the transcriptional repressor Foxp3 as a specific marker gene (38, 39). A link between T reg cells and a membrane complement regulatory protein was demonstrated in a recent study whereby coengagement of CD3 and the complement regulator CD46, in the presence of IL-2, induced an IL-10–secreting T reg cell phenotype in human CD4$^+$ T cells (40). We found no defect in naive Daf1$^{-/-}$ mice with regard to the number or function of their naturally occurring T reg cells (Fig. 6, E–G). Although the reduced production of IL-10 by Daf1$^{-/-}$ lymphocytes would be compatible with the hypothesis of impaired differentiation or function of IL-10–secreting T reg cells, it remains to be established whether the defect in IL-10 production originated from T reg cells or other IL-10–secreting cells such as macrophages. An argument against the impaired IL-10–secreting T reg cell hypothesis is the observation that C3 deficiency rescued the hyper T cell response phenotype of Daf1$^{-/-}$ mice but did not consistently correct their IL-10 defect, suggesting that reduced IL-10 production was not central to the Daf1$^{-/-}$ mouse phenotype.

The notion that DAF suppresses T cell immunity through complement regulation either locally (on T cells, APCs, or in tissue microenvironments) or systemically has several clinical implications. For example, transgenic expression of human DAF on porcine endothelial cells is used as a strategy to circumvent complement-mediated hyperacute rejection in xenotransplantation (9–11). Our findings here suggest that such a strategy may have the added benefit of suppressing T cell–mediated acute or chronic rejection. In a separate clinical setting, expression of DAF is up-regulated on many types of human tumors and this has been interpreted as conferring an advantage to the tumor cells in their resistance to complement lysis (6–8). We suggest that a more significant ramification of DAF overexpression on tumor cells might be that it provides protection from T cell–mediated tumorecidal activity. In this context, it is of interest to note that two tumor-associated antigens, 791Tgp72 and SC-1 antigen, which had been used successfully as targets for tumor imaging and T cell or antibody immunotherapy in Phase I and II clinical trials, respectively, were recently identified as DAF (41, 42). Finally, the markedly enhanced memory T cell response phenotype in Daf1$^{-/-}$ mice raises the prospect that DAF might be exploited as a therapeutic target for effective vaccine development.

MATERIALS AND METHODS

Mice. We studied 6–8-wk-old male C57BL/6-Df1$^{-/-}$ and BALB/c-Daf1$^{-/-}$ mice. Two DAF genes, Daf1 and Daf2, are present in the mouse (43, 44). Daf1 encodes a GPI-anchored DAF protein and is widely expressed on mouse tissues (43–45). Daf2 is predominantly expressed in the mouse testis and its major transcript encodes a transmembrane form of DAF (43–45). The Daf1$^{-/-}$ mouse was generated by gene targeting as described previously (19). The mouse was subsequently backcrossed for nine generations with C57BL/6 or BALB/c mice to derive either the C57BL/6-Df1$^{-/-}$ or BALB/c-Daf1$^{-/-}$ mice used in this investigation. No alteration in the expression of Daf2 or two other membrane complement regulators, CD59a and Crry, was observed on blood cells or several tissues examined in these Daf1$^{-/-}$ mice (19, 20, 22, 46; unpublished data). Gender- and age-matched WT C57BL/6 and BALB/c mice were obtained from The Jackson Laboratory. Six time-backcrossed C57BL/6-C3$^{-/-}$ mice were obtained from The Jackson Laboratory. These mice were backcrossed for one more generation in our colony to derive the seven time-backcrossed C57BL/6-C3$^{-/-}$ mice used in this study. C57BL/6-Df1$^{-/-}$-C3$^{-/-}$ mice were generated by crossing nine time-backcrossed C57BL/6-Df1$^{-/-}$ mice with seven time-backcrossed C57BL/6-C3$^{-/-}$ mice. Mice were housed in a specific pathogen-free facility and all experimental protocols were approved by the Institutional Animal Care and Use Committee of the University of Pennsylvania.

Reagents. Chicken OVA was from Difco Laboratories. Mouse MOG 38–50 peptide was synthesized and purified on HPLC by Research Genetics. Pertussis toxin was from List Biological Laboratories. SEB was from Toxin Technology Inc. CFA, [^{3}H]thymidine, gelatin veronal-buffered saline (GVBS)$^{2+}$, and PE-goat anti–rabbit IgG were from Sigma-Aldrich. A monoclonal rat anti–mouse CD59a (47) was provided by P. Morgan (University of Wales, Cardiff, UK). Two hamster anti–mouse DAF mAbs, Riko-3 and Riko-4 (48), were provided by N. Okada (Nagoya City University, Nagoya, Japan). A polyclonal rabbit anti–mouse Crry was provided by M. Holers (University of Colorado Health Sciences Center, Denver, CO). FITC-donkey anti–rat IgG ([Fab′]$_2$) was from Jackson ImmunoResearch Laboratories. PE-goat anti–hamster IgG, purified hamster anti–mouse CD3e (clone 145-2C11), APCcy7-rat anti–mouse CD4, PE-rat anti–mouse CD8, FITC-hamster anti–mouse CD69, and FITC-rat anti–mouse CD25 were from BD Biosciences. Microbead-conjugated antibodies against CD4, CD8, CD19, CD90, and DX5 were from Miltenyi Biotec. Quantitative ELISA kits for mouse IFN-γ, IL-2, IL-4, and IL-10 were from BD Biosciences. The anti–mouse C5 hybridoma (BB5.1) was originally generated by immunization of a C5-deficient mouse as described previously (49). Mouse ascites for the anti-C5 mAb were produced by Cocalico Biologicals Inc. The anti-C5 mAb was partially purified from mouse ascites using the caprylic acid method, involving ammonium sulfate precipitation followed by dialysis (50). An isotype control mAb (MOPC21, IgG1, lyophilized protein) was from Sigma-Aldrich. It was resuspended in PBS before use.

Mouse immunization. Mice were immunized by subcutaneous injection in the flank with 100 μg OVA or 300 μg MOG 38–50 peptide emulsified in an equal volume of CFA. 12 d later, inguinal and axillary LNs and/or spleens were collected for single cell preparation used in antigen restimulation assays in vitro. For memory T cell response, antigen restimulation assays were performed 60–110 d after immunization.

Anti-C5 mAb treatment. C57BL/6-Df1$^{-/-}$ mice were treated with the anti-C5 mAb or the isotype-matched IgG control antibody (1 mg/mouse, i.p.) every 4 d starting from 1 d before OVA immunization. As a separate control group, C57BL/6 WT mice were treated with the isotype-matched IgG control antibody. C5 depletion in the anti-C5 mAb-treated mice was confirmed by testing the relative hemolytic activities of their sera collected at day 4 after anti-C5 mAb treatment using antibody-sensitized RBCs from Daf1$^{-/-}$/Crry$^{-/-}$/C3$^{-/-}$ triple knockout mice (51). In brief, RBCs from Daf1$^{-/-}$/Crry$^{-/-}$/C3$^{-/-}$ mice (2–3 × 10^7 cells in a 100-μl volume of GVBS^{2+}) were sensitized with 10 mg/ml 34-3C, a murine anti-erythrocyte

monoclonal autoantibody (46). After washing twice with PBS and once with $GVBS^{2+}$, the sensitized RBCs were exposed to the assay sera at 1:10 or 1:5 in $GVBS^{2+}$ for 30 min at 37°C. The percent RBC lysis was estimated by measuring the OD value of the supernatant at 414 nm as described previously (46). Using this assay, we found that <10% of the hemolytic activity remained at day 4 in mice receiving a single anti-C5 injection. In contrast, the hemolytic activity of mice receiving the control IgG antibody remained similar to that of untreated mice.

Antigen restimulation of lymphocytes in vitro. For cytokine assays, LN cells or a mixture of LN cells and splenocytes from immunized mice were cultured at 1.5×10^6 cells/well in 0.2 ml DMEM (Life Technologies) containing 10% FBS, 2 mM L-glutamine, 10 mM Hepes, 0.1 mM nonessential amino acids, 100 U penicillin-streptomycin, 50 μM 2-mercaptoethanol, and 1 mM sodium pyruvate. Cells were stimulated with 0, 5, and 25 μg/ml OVA or MOG 38–50. Cell culture supernatants were collected at 40 (for IFN-γ assay) or 96 h (for IL-2, IL-4, and IL-10 assay). For T cell proliferation assays, LN cells were seeded at 0.5×10^6 cells/well. After 48 h, [^{3}H]thymidine (1 μCi/well) was added to the culture medium, and the cells were harvested 16 h later. Cellular incorporation of radioactivity was determined using a flatbed β counter (Wallac).

SEB stimulation of lymphocytes in vitro. To assess the general sensitivity of Daf1$^{-/-}$ mouse T cells to activation stimuli, splenocytes were prepared from naive C57BL/6 WT and Daf1$^{-/-}$ mice and were stimulated with the bacterial superantigen SEB. Cells were plated at 1.0×10^6 cells/well in 96-well, round-bottom culture plates and stimulated with SEB (1 pg/ml to 100 ng/ml) in a final volume of 0.2 ml medium. Expression of the early activation marker CD69 on $CD4^+$ and $CD8^+$ T cells was examined at 18 h by FACS after three-color staining with APCcy7–anti-CD4, PE–anti-CD8, and FITC–anti-CD69. In parallel experiments, cell culture supernatants were collected at 40 h to determine IFN-γ production. For proliferation assays, splenocytes were plated at 0.5×10^6 cells/well and stimulated with SEB as described above for 48 h and then pulsed with [^{3}H]thymidine (1 μCi/well). They were cultured for another 16 h before being harvested.

Purification of $CD4^+$ T cells and APCs. $CD4^+$ T cells were isolated by two rounds of selection. First, a $CD4^+$ T cell–enriched cell population was isolated from combined LN cells and splenocytes of immunized mice by negative selection using a magnetic bead–based $CD4^+$ T cell isolation kit (Miltenyi Biotec). These cells were then stained with FITC-conjugated anti-CD4 and positive cells were subsequently selected by FACS. The purity of $CD4^+$ T cells prepared in this manner was consistently >99%. APCs were purified from the same source of spleen and LN cells by negative selection using mAbs against mouse CD4, CD8, CD19, CD90, as well as anti-NK cells (DX5) and an autoMACS cell sorter (Miltenyi Biotec).

Analysis of T reg cell number and function. Splenocytes from naive C57BL/6 WT and Daf1$^{-/-}$ mice were stained for CD4 and CD25, and the percentage of $CD25^+$ cells in the $CD4^+$ T cell population was determined after FACS analysis. The number of naturally occurring T reg cells was estimated by real-time RT-PCR analysis of Foxp3, a marker gene specifically expressed in T reg cells. For this experiment, $CD4^+$ T cells were purified by negative selection from splenocytes (three samples in each genotype, with each sample representing splenocytes pooled from two mice) as described above. Total RNAs were extracted from 10^6 $CD4^+$ cells using 1 ml TRIzol reagent (Invitrogen Life Technologies), and first strand cDNA was synthesized by reverse transcription using random hexamer primers. Foxp3 mRNA was quantified using the ABI 7900 Real-Time PCR System (Applied Biosystems). Amplification was performed in a total volume of 15 μl for 40 cycles, and products were detected using SYBR Green I dye (Applied Biosystems). Samples were run in duplicate and relative expression level was determined by normalization to the housekeeping gene L32 (52) with results presented as relative expression units. Primer sequences used were as follows: L32, forward: 5′-GGAAACCCAGAGGCATTGAC-3′, reverse: 5′-TCAGGATCTGGCCCTTGAAC-3′; Foxp3, forward: 5′-GGCCCTTCTCCAGGACAGA-3′, reverse: 5′-GCTGATCATGGCTGGGTTGT-3′.

To assess T reg cell function, the abilities of $CD4^+$ $CD25^+$ T cells from WT and Daf1$^{-/-}$ mice to inhibit anti-CD3–stimulated proliferation of $CD4^+$ $CD25^-$ T cells were compared. $CD4^+$ T cells were first purified from splenocytes (pooled from six mice in each genotype) by negative selection as described above. After staining with FITC–anti-CD25, $CD4^+$ $CD25^+$ and $CD4^+$ $CD25^-$ T cells were separated by FACS sorting. For functional assays, $CD4^+$ $CD25^+$ T cells (5×10^4 cells /well) from WT or Daf1$^{-/-}$ mice were mixed with equal numbers of $CD4^+$ $CD25^-$ T cells and irradiated splenocytes (both from C57BL/6 WT mice). Triplicate assays were performed for each treatment group. The cells were stimulated for 72 h with 500 ng/ml anti-CD3, and [^{3}H]thymidine (1 μCi /well) was added 16 h before cell harvest. Cellular incorporation of radioactivity was determined using a flatbed β counter (Wallac).

ELISPOT assay. IFN-γ ELISPOT assay was performed using an ELISPOT kit from BD Biosciences. In brief, 96-well plates were coated overnight at 4°C with a capture antibody (5.0 μg/ml anti–mouse IFN-γ). After blocking for 2 h, the plates were washed three times with PBS. LN cells and splenocytes were seeded at 10^5 cells/well and cultured for 40 h. After removing the cells, the plates were washed extensively with PBS/0.05% Tween-20, and 2.0 μg/ml of a detection antibody, biotinylated anti–mouse IFN-γ, was then added. After incubating at room temperature for 2 h, the plates were washed again and incubated with Streptavidin–horseradish peroxidase for 1 h before being developed by addition of the horseradish peroxidase substrate. The plates were then analyzed using the ImmunoSpot Analyzer and associated software to determine the number, size, and colorimetric density of positive spots.

Induction of EAE. Mice were immunized by subcutaneous injection in the flank with 300 μg MOG 38–50 in 0.1 ml PBS emulsified in an equal volume of CFA containing 5 mg/ml *Mycobacterium tuberculosis* H37RA (Difco Laboratories). Pertussis toxin (100 ng/mouse) was administered intravenously on the day of immunization and 2 d later. Mice were examined daily for signs of EAE and scored as follows: 0, no disease; 1, tail paralysis; 2, hind limb weakness; 3, hind limb paralysis; 4, hind limb plus forelimb paralysis; and 5, moribund or dead.

Histological studies. Mice were perfused with PBS and 10% formalin phosphate. Spinal cords were embedded in paraffin, cut into five pieces, and then sectioned at 5 μm and stained with hematoxylin and eosin or with luxol fast blue, a myelin-specific stain. The degree of inflammation and demyelination in spinal cords was assessed by estimating the percentage of tissue section areas that were infiltrated by inflammatory cells or negative for myelin staining. From each animal, a total of 10 tissue sections from the cervical, thoracic, lumbar, and sacral spinal cord were examined in a blind fashion.

We thank Drs. Paul Morgan, Michael Holers, and Noriko Okada for kindly providing antibodies for CD59a, Crry, and DAF; Dr. Michele Kutzler for help in ELISPOT analysis; and Bethany Everson for manuscript preparation.

This work is supported by grants AI-44970 and AI-49344 from the National Institute of Allergy and Infectious Diseases (to W.-C. Song) and GM-62134 from the National Institute of General Medical Sciences (to J.D. Lambris).

The authors have no conflicting financial interests.

Submitted: 3 May 2004
Accepted: 21 December 2004

REFERENCES

1. Lublin, D.M., and J.P. Atkinson. 1989. Decay-accelerating factor: biochemistry, molecular biology, and function. *Annu. Rev. Immunol.* 7:35–58.
2. Miwa, T., and W.C. Song. 2001. Membrane complement regulatory proteins: insight from animal studies and relevance to human diseases. *Int. Immunopharmacol.* 1:445–459.

3. Nicholson-Weller, A., J.P. March, S.I. Rosenfeld, and K.F. Austen. 1983. Affected erythrocytes of patients with paroxysmal nocturnal hemoglobinuria are deficient in the complement regulatory protein, decay accelerating factor. *Proc. Natl. Acad. Sci. USA.* 80:5066–5070.
4. Pangburn, M.K., R.D. Schreiber, and H.J. Muller-Eberhard. 1983. Deficiency of an erythrocyte membrane protein with complement regulatory activity in paroxysmal nocturnal hemoglobinuria. *Proc. Natl. Acad. Sci. USA.* 80:5430–5434.
5. Rosse, W.F., and C.J. Parker. 1985. Paroxysmal nocturnal haemoglobinuria. *Clin. Haematol.* 14:105–125.
6. Cheung, N.K., E.I. Walter, W.H. Smith-Mensah, W.D. Ratnoff, M.L. Tykocinski, and M.E. Medof. 1988. Decay-accelerating factor protects human tumor cells from complement-mediated cytotoxicity in vitro. *J. Clin. Invest.* 81:1122–1128.
7. Li, L., I. Spendlove, J. Morgan, and L.G. Durrant. 2001. CD55 is overexpressed in the tumour environment. *Br. J. Cancer.* 84:80–86.
8. Fishelson, Z., N. Donin, S. Zell, S. Schultz, and M. Kirschfink. 2003. Obstacles to cancer immunotherapy: expression of membrane complement regulatory proteins (mCRPs) in tumors. *Mol. Immunol.* 40:109–123.
9. McCurry, K.R., D.L. Kooyman, C.G. Alvarado, A.H. Cotterell, M.J. Martin, J.S. Logan, and J.L. Platt. 1995. Human complement regulatory proteins protect swine-to-primate cardiac xenografts from humoral injury. *Nat. Med.* 1:423–427.
10. Schuurman, H.J., G. Pino-Chavez, M.J. Phillips, L. Thomas, D.J. White, and E. Cozzi. 2002. Incidence of hyperacute rejection in pig-to-primate transplantation using organs from hDAF-transgenic donors. *Transplantation.* 73:1146–1151.
11. Lavitrano, M., M.L. Bacci, M. Forni, D. Lazzereschi, C. Di Stefano, D. Fioretti, P. Giancotti, G. Marfe, L. Pucci, L. Renzi, et al. 2002. Efficient production by sperm-mediated gene transfer of human decay accelerating factor (hDAF) transgenic pigs for xenotransplantation. *Proc. Natl. Acad. Sci. USA.* 99:14230–14235.
12. Davis, L.S., S.S. Patel, J.P. Atkinson, and P.E. Lipsky. 1988. Decay-accelerating factor functions as a signal transducing molecule for human T cells. *J. Immunol.* 141:2246–2252.
13. Shenoy-Scaria, A.M., J. Kwong, T. Fujita, M.W. Olszowy, A.S. Shaw, and D.M. Lublin. 1992. Signal transduction through decay-accelerating factor. Interaction of glycosyl-phosphatidylinositol anchor and protein tyrosine kinases p56lck and p59fyn 1. *J. Immunol.* 149:3535–3541.
14. Tosello, A.C., F. Mary, M. Amiot, A. Bernard, and D. Mary. 1998. Activation of T cells via CD55: recruitment of early components of the CD3-TCR pathway is required for IL-2 secretion. *J. Inflamm.* 48:13–27.
15. Hamann, J., W. Eichler, D. Hamann, H.M. Kerstens, P.J. Poddighe, J.M. Hoovers, E. Hartmann, M. Strauss, and R.A. van Lier. 1995. Expression cloning and chromosomal mapping of the leukocyte activation antigen CD97, a new seven-span transmembrane molecule of the secretion receptor superfamily with an unusual extracellular domain. *J. Immunol.* 155:1942–1950.
16. Gray, J.X., M. Haino, M.J. Roth, J.E. Maguire, P.N. Jensen, A. Yarme, M.A. Stetler-Stevenson, U. Siebenlist, and K. Kelly. 1996. CD97 is a processed, seven-transmembrane, heterodimeric receptor associated with inflammation. *J. Immunol.* 157:5438–5447.
17. Hamann, J., B. Vogel, G.M. van Schijndel, and R.A. van Lier. 1996. The seven-span transmembrane receptor CD97 has a cellular ligand (CD55, DAF). *J. Exp. Med.* 184:1185–1189.
18. Qian, Y.M., M. Haino, K. Kelly, and W.C. Song. 1999. Structural characterization of mouse CD97 and study of its specific interaction with the murine decay-accelerating factor (DAF, CD55). *Immunology.* 98:303–311.
19. Sun, X., C.D. Funk, C. Deng, A. Sahu, J.D. Lambris, and W.C. Song. 1999. Role of decay-accelerating factor in regulating complement activation on the erythrocyte surface as revealed by gene targeting. *Proc. Natl. Acad. Sci. USA.* 96:628–633.
20. Sogabe, H., M. Nangaku, Y. Ishibashi, T. Wada, T. Fujita, X. Sun, T. Miwa, M.P. Madaio, and W.C. Song. 2001. Increased susceptibility of decay-accelerating factor deficient mice to anti-glomerular basement membrane glomerulonephritis. *J. Immunol.* 167:2791–2797.
21. Yamada, K., T. Miwa, J. Liu, M. Nangaku, and W.C. Song. 2004. Critical protection from renal ischemia reperfusion injury by CD55 and CD59. *J. Immunol.* 172:3869–3875.
22. Miwa, T., M.A. Maldonado, L. Zhou, X. Sun, H.Y. Luo, D. Cai, V.P. Werth, M.P. Madaio, R.A. Eisenberg, and W.C. Song. 2002. Deletion of decay-accelerating factor (CD55) exacerbates autoimmune disease development in MRL/lpr mice. *Am. J. Pathol.* 161:1077–1086.
23. Hilliard, B., A. Wilmen, C. Seidel, T.S. Liu, R. Goke, and Y. Chen. 2001. Roles of TNF-related apoptosis-inducing ligand in experimental autoimmune encephalomyelitis. *J. Immunol.* 166:1314–1319.
24. Girardi, G., J. Berman, P. Redecha, L. Spruce, J.M. Thurman, D. Kraus, T.J. Hollmann, P. Casali, M.C. Caroll, R.A. Wetsel, et al. 2003. Complement C5a receptors and neutrophils mediate fetal injury in the antiphospholipid syndrome. *J. Clin. Invest.* 112:1644–1654.
25. Mead, R.J., J.W. Neal, M.R. Griffiths, C. Linington, M. Botto, H. Lassmann, and B.P. Morgan. 2004. Deficiency of the complement regulator CD59a enhances disease severity, demyelination and axonal injury in murine acute experimental allergic encephalomyelitis. *Lab. Invest.* 84:21–28.
26. Calida, D.M., C. Constantinescu, E. Purev, G.X. Zhang, E.S. Ventura, E. Lavi, and A. Rostami. 2001. Cutting edge: C3, a key component of complement activation, is not required for the development of myelin oligodendrocyte glycoprotein peptide-induced experimental autoimmune encephalomyelitis in mice. *J. Immunol.* 166:723–726.
27. Carroll, M.C. 2000. The role of complement in B cell activation and tolerance. *Adv. Immunol.* 74:61–88.
28. Fearon, D.T., and M.C. Carroll. 2000. Regulation of B lymphocyte responses to foreign and self-antigens by the CD19/CD21 complex. *Annu. Rev. Immunol.* 18:393–422.
29. Walport, M.J. 2001. Complement. First of two parts. *N. Engl. J. Med.* 344:1058–1066.
30. Stager, S., J. Alexander, A.C. Kirby, M. Botto, N.V. Rooijen, D.F. Smith, F. Brombacher, and P.M. Kaye. 2003. Natural antibodies and complement are endogenous adjuvants for vaccine-induced CD8+ T-cell responses. *Nat. Med.* 9:1287–1292.
31. Kopf, M., B. Abel, A. Gallimore, M. Carroll, and M.F. Bachmann. 2002. Complement component C3 promotes T-cell priming and lung migration to control acute influenza virus infection. *Nat. Med.* 8:373–378.
32. Pratt, J.R., S.A. Basheer, and S.H. Sacks. 2002. Local synthesis of complement component C3 regulates acute renal transplant rejection. *Nat. Med.* 8:582–587.
33. Suresh, M., H. Molina, M.S. Salvato, D. Mastellos, J.D. Lambris, and M. Sandor. 2003. Complement component 3 is required for optimal expansion of CD8 T cells during a systemic viral infection. *J. Immunol.* 170:788–794.
34. Sadlack, B., J. Lohler, H. Schorle, G. Klebb, H. Haber, E. Sickel, R.J. Noelle, and I. Horak. 1995. Generalized autoimmune disease in interleukin-2-deficient mice is triggered by an uncontrolled activation and proliferation of CD4+ T cells. *Eur. J. Immunol.* 25:3053–3059.
35. Nishimura, H., T. Okazaki, Y. Tanaka, K. Nakatani, M. Hara, A. Matsumori, S. Sasayama, A. Mizoguchi, H. Hiai, N. Minato, and T. Honjo. 2001. Autoimmune dilated cardiomyopathy in PD-1 receptor-deficient mice. *Science.* 291:319–322.
36. Miwa, T., X. Sun, R. Ohta, N. Okada, C.L. Harris, B.P. Morgan, and W.C. Song. 2001. Characterization of glycosylphosphatidylinositol-anchored decay accelerating factor (GPI-DAF) and transmembrane DAF gene expression in wild-type and GPI-DAF gene knockout mice using polyclonal and monoclonal antibodies with dual or single specificity. *Immunology.* 104:207–214.
37. Lin, F., Y. Fukuoka, A. Spicer, R. Ohta, N. Okada, C.L. Harris, S.N. Emancipator, and M.E. Medof. 2001. Tissue distribution of products of the mouse decay-accelerating factor (DAF) genes. Exploitation of a Daf1 knock-out mouse and site-specific monoclonal antibodies. *Immunology.* 104:215–225.
38. O'Garra, A., and P. Vieira. 2004. Regulatory T cells and mechanisms of immune system control. *Nat. Med.* 10:801–805.
39. Vieira, P.L., J.R. Christensen, S. Minaee, E.J. O'Neill, F.J. Barrat, A. Boonstra, T. Barthlott, B. Stockinger, D.C. Wraith, and A. O'Garra. 2004. IL-10-secreting regulatory T cells do not express Foxp3 but have

comparable regulatory function to naturally occurring CD4+CD25+ regulatory T cells. *J. Immunol.* 172:5986–5993.
40. Kemper, C., A.C. Chan, J.M. Green, K.A. Brett, K.M. Murphy, and J.P. Atkinson. 2003. Activation of human CD4+ cells with CD3 and CD46 induces a T-regulatory cell 1 phenotype. *Nature.* 421:388–392.
41. Spendlove, I., L. Li, J. Carmichael, and L.G. Durrant. 1999. Decay accelerating factor (CD55): a target for cancer vaccines? *Cancer Res.* 59: 2282–2286.
42. Hensel, F., R. Hermann, C. Schubert, N. Abe, K. Schmidt, A. Franke, A. Shevchenko, M. Mann, H.K. Muller-Hermelink, and H.P. Vollmers. 1999. Characterization of glycosylphosphatidylinositol-linked molecule CD55/decay-accelerating factor as the receptor for antibody SC-1-induced apoptosis. *Cancer Res.* 59:5299–5306.
43. Spicer, A.P., M.F. Seldin, and S.J. Gendler. 1995. Molecular cloning and chromosomal localization of the mouse decay-accelerating factor genes. Duplicated genes encode glycosylphosphatidylinositol-anchored and transmembrane forms. *J. Immunol.* 155:3079–3091.
44. Song, W.C., C. Deng, K. Raszmann, R. Moore, R. Newbold, J.A. McLachlan, and M. Negishi. 1996. Mouse decay-accelerating factor: selective and tissue-specific induction by estrogen of the gene encoding the glycosylphosphatidylinositol-anchored form. *J. Immunol.* 157: 4166–4172.
45. Harris, C.L., N.K. Rushmere, and B.P. Morgan. 1999. Molecular and functional analysis of mouse decay accelerating factor (CD55). *Biochem. J.* 341:821–829.
46. Miwa, T., L. Zhou, B. Hilliard, H. Molina, and W.C. Song. 2002. Crry, but not CD59 and DAF, is indispensable for murine erythrocyte protection in vivo from spontaneous complement attack. *Blood.* 99: 3707–3716.
47. Harris, C.L., S.M. Hanna, M. Mizuno, D.S. Holt, K.J. Marchbank, and B.P. Morgan. 2003. Characterization of the mouse analogues of CD59 using novel monoclonal antibodies: tissue distribution and functional comparison. *Immunology.* 109:117–126.
48. Ohta, R., M. Imai, Y. Fukuoka, T. Miwa, N. Okada, and H. Okada. 1999. Characterization of mouse DAF on transfectant cells using monoclonal antibodies which recognize different epitopes. *Microbiol. Immunol.* 43:1045–1056.
49. Frei, Y., J.D. Lambris, and B. Stockinger. 1987. Generation of a monoclonal antibody to mouse C5 application in an ELISA assay for detection of anti-C5 antibodies. *Mol. Cell. Probes.* 1:141–149.
50. Harlow, E., and D. Lane. 1988. Antibodies: A Laboratory Manual. Cold Spring Harbor Laboratory, Cold Spring Harbor, NY. 726 pp.
51. Molina, H., T. Miwa, L. Zhou, B. Hilliard, D. Mastellos, M.A. Maldonado, J.D. Lambris, and W.C. Song. 2002. Complement-mediated clearance of erythrocytes: mechanism and delineation of the regulatory roles of Crry and DAF. Decay-accelerating factor. *Blood.* 100:4544–4549.
52. Polanczyk, M.J., B.D. Carson, S. Subramanian, M. Afentoulis, A.A. Vandenbark, S.F. Ziegler, and H. Offner. 2004. Cutting edge: estrogen drives expansion of the CD4+CD25+ regulatory T cell compartment. *J. Immunol.* 173:2227–2230.